An experimental study of multimodal glass suspension rheology to test and validate a polydisperse suspension viscosity model

P. Masafu Mwasame[1], Cameron A. Mertz[1], Evan J. Rosario[2], Antony N. Beris[1] and Norman J. Wagner [1,a)]

[1]Department of Chemical and Biomolecular Engineering, University of Delaware, Newark, DE 19716

[2]Appoquinimink High School, Middletown, DE 19709

Rheological Acta

Experimental measurements of noncolloidal multimodal suspension viscosities are performed over a wide range of mixing ratios and used to test the robustness and predictive capability of a recent viscosity model (Phys. Fluids 28, 061701, 2016), subsequently referred to as the MWB model. Three unimodally-distributed particle suspensions with narrow size distributions are blended to make the bimodal and trimodal suspensions used in the rheological experiments. We demonstrate how predictions for mixture viscosities can be made using the MWB model only requiring the volume-weighted average particle sizes and viscosity correlations of the individual unimodal suspensions comprising the blend. The resultant model predictions are found to be in good agreement with measured bimodal and trimodal viscosity data to within expected experimental uncertainty. The datasets provided here can be used to validate future modeling efforts and the MWB model can be used to optimize the viscosity of multimodal suspension mixtures for specific performance criteria.

[a)]Corresponding Author. Tel. 1-302-831-8079, E-mail address: wagnernj@udel.edu

INTRODUCTION

Modeling the rheological behavior of suspensions comprising of more than one particle size, i.e., polydisperse suspensions, is a long-standing problem of interest in suspension rheology (Mooney 1951, Farris 1968, Chong *et al.* 1971). Polydisperse suspensions are encountered in a broad range of processes with industrial and consumer relevance ranging from coal slurries to concrete mixes to tooth fillings. The ability to model the viscosity behavior of polydisperse suspensions has many applications in industry; e.g. determining the maximum loading for which a suspension can still flow. With more particles suspended/dispersed in the fluid, more of a desired industrial product can be transported in a suspended state and still flow. This is especially pertinent in the pipeline transport, where profitability can strongly depend on pumping the most/optimum amount of suspended material. Therefore, the determination of the maximum tolerable viscosity of a suspension corresponding to an optimum particle loading, by using carefully tailored size distributions, is an industrially relevant problem.

Recently there has been a renewed interest in developing improved models to account for the effects of polydispersity on the rheology of suspensions (Qi and Tanner 2012, Dörr *et al.* 2013, Farr 2014, Faroughi and Huber 2014, Shewan and Stokes 2015, Mwasame *et al.* 2016a, Mwasame *et al.* 2016b). Recently, Mwasame *et al.* (2016a, 2016b) described an extension of the Farris approach (Farris 1968), henceforth referred to as the MWB model, to account for polydispersity effects in binary as well as truly polydisperse suspensions and compared it to a number of models available in the literature. The MWB model is a semi-empirical model allowing it to capture experimental artefacts responsibly for deviations from hard sphere suspension behavior without requiring apriori knowledge of these e.g. those arising from physico-chemical details of the suspended particles. This robustness arises because the only input required to apply the MWB model to predict polydisperse suspensions viscosity is the monodisperse viscosity correlation of the constituent particles of the polydisperse suspension under consideration (Mwasame *et al.* 2016a, 2016b). Other advantages of the MWB model include its capability to reproducing all known limiting suspension behaviors (Mwasame *et al.* 2016b) and its applicability to any arbitary combinations of particle sizes and volume fractions, avoiding inherent limitations of some existing models (Furnas 1931; Farris 1968; Ouchiyama 1984).

The MWB model was originally developed to predict the viscosity of polydisperse suspensions that have been formulated by mixing monodisperse particle sizes. For example, a binary suspension comprises of two distinct particle sizes, d, and D each comprising of a volume fraction ϕ_d and ϕ_D. To facilitate the evaluation of the viscosity of a binary suspension, a fraction of the small particles, denoted by volume fraction ϕ_d, is considered together with the suspending medium to form an effective medium

whose viscosity is defined as $\eta_{r,eff} \equiv \mu\eta_r\left(\phi_d/(1-(1-\mathrm{f})\phi_D),\phi_{\max}\right)(1-f)$. In this expression, μ is the suspending medium viscosity and the expression for $\eta_r\left(x,\phi_{\max}\right)$ can be defined based on any one of the available semi-empirical viscosity correlations available in the literature, see for example Wagner & Mewis (2012). In the same expression, f is defined as a hydrodynamic factor that takes on values between zero and one. Furthermore, it is important to note that the expression for $\eta_{r,eff}$ generalizes the results of Farris (1968) through the factor $(1-f)$ that weights the viscosity contribution. The factor f is defined to have a limiting value of zero when the relative size difference is very large i.e., $d/D \ll 1$ in agreement with the important results of Farris (1968). In this "Farris" limit, the small size d particles in the suspension simply act to enhance the background viscosity that is experienced by the larger size D particles.

In many applications, the primary interest is to predict the viscosity of suspensions with "interfering" particle sizes, i.e., $0.1 < d/D \leq 1$. Consequently, Mwasame et al. (2016a) deemed it necessary to define the hydrodynamic weighting function f in the MWB model to be a function of both the size ratio and relative composition of the particles comprising the binary suspension. Subsequently to fully account for the interference effects between small and large particles when $0.1 < d/D \leq 1$, a second renormalization step was proposed such that a fraction of small particles, $f\phi_d$, is considered to behave as effective larger size D particle such that the total effective volume fraction of the large particles becomes $f\phi_d + \phi_D$. Subsequently, the total binary suspension viscosity $\eta_{r,bi}$ is then obtained in a multiplicative fashion as the product of the effective medium viscosity $\eta_{r,eff}$ and the effective relative viscosity of the large particles, based on the effective volume fraction of $(1-f)\phi_d + \phi_D$, as $\eta_{r,bi} = \eta_{r,eff}\eta_r\left(f\phi_d + \phi_D, \phi_{\max}\right)$. In an analogous fashion, an expression for the viscosity of a ternary suspension that is formulated as a blend of three distinct monodisperse particle sizes can also be derived by employing a sequence of two renormalization steps and defining two hydrodynamic weighting functions, both with the same functional form (Mwasame *et al.* 2016b). As a result, the hydrodynamic functions in the extension of the MWB model to ternary suspensions employ the same set of parameters that is used in the definition of the binary suspension hydrodynamic function. This is a powerful feature of the MWB model that allows for its use in a predictive fashion once parameterized based on binary suspension data. Additional details on the calculation of binary and ternary suspension viscosities using the MWB model are described in Mwasame *et al.* (2016a, 2016b). An important result arising from subsequent development of the extension of the MWB model to polydisperse suspensions is that only six

moments are required to accurately represent such systems. In other words, polydisperse suspensions can be accurately approximated as equivalent ternary suspensions in the context of the MWB model (Mwasame *et al.* 2016a).

A key feature of the MWB model is that once parameterized, based on binary suspension data alone, it can be systematically extended to multimodal and polydisperse suspensions without the need for additional model parameters. The MWB model parameters have been determined empirically (Mwasame *et al.* 2016b) based on experimental results of Chang and Powell (1994) and Chong *et al.* (1971). Such an empirical parameterization was favored as existing theoretical results are limited to the dilute limit (Wagner and Woutersen 1994) in which the effects of polydispersity on suspension viscosity are mild. Once a parameterization of the model is selected, the only system-independent information required by the model is the monodisperse viscosity correlations, η_r, of the particle sizes that are mixed to form the final binary, ternary or polydisperse suspensions. Such a provision to allow for the empirical determination of η_r is reasonable as the viscosity of rigid spheres, especially at high volume fractions, is very sensitive to microscopic details e.g. surface roughness, interactions, and nanoscale effects (Mewis and Wagner 2012).

In this work, we seek to examine the predictive capability of the MWB model when applied to mixed unimodal suspensions that more closely resemble suspensions encountered in practice. An experimental design is constructed to critically test the predictive capability of the MWB model. Applying the model to real world suspension mixtures requires approximations of the unimodal suspensions as monodisperse suspensions. This is accomplished through a two-step process: (1) the 'average size' of the equivalent monodisperse suspension is described by the volume weighted average size of the unimodal suspension (Wagner and Woutersen 1994, Mwasame *et al.* 2016a), and (2) If necessary, each equivalent suspension can be handled in the MWB model through a unique monodisperse viscosity correlation for the case of suspensions exhibiting size-dependent monodisperse viscosities (Mwasame *et al.* 2016b). The 'coarse-graining' approach in (1) is useful and emerges as a natural extension to apply the MWB model in non-ideal situations where the polydisperse suspension is constructed from unimodal suspensions instead of truly monodisperse suspensions.

In the following manuscript, we present the procedure of coarse-graining a unimodal size distribution as an equivalent monodisperse distribution. Then, we describe the materials as well as rheological and characterization techniques applied to the three unimodal suspensions used in this work. Next, the experimentally measured particle sizing information on the various unimodal suspensions that is used to determine the volume weighted particle sizes are presented along with the experimentally

measured viscosities of the unimodal, bimodal and trimodal suspensions. Comparisons with model predictions of the bimodal and trimodal suspension viscosities using the MWB model (and viscosity correlations obtained from the measured unimodal suspension viscosities) are then discussed before the conclusions are presented.

COARSE-GRAINING UNIMODAL SIZE DISTRIBUTIONS

The MWB model was originally developed to describe binary, ternary and multi-n-ary suspension made from blending ideal monodisperse suspensions. However, in this work, we seek to apply the model to describe the viscosity of bimodal suspensions that are formulated from blends of unimodal, but not monodisperse suspensions. The difference between a binary distributed suspension (comprising of two constituent monodisperse particle sizes) and a bimodally distributed suspension (comprising of two constituent unimodal particle size distributions) is depicted in Fig. 1. For clarity, the procedure to apply the MWB model to predict binary suspension viscosity is first summarized and the proposed necessary coarse-graining of the underlying unimodal distributions so as to predict bimodal suspension viscosities is subsequently elaborated.

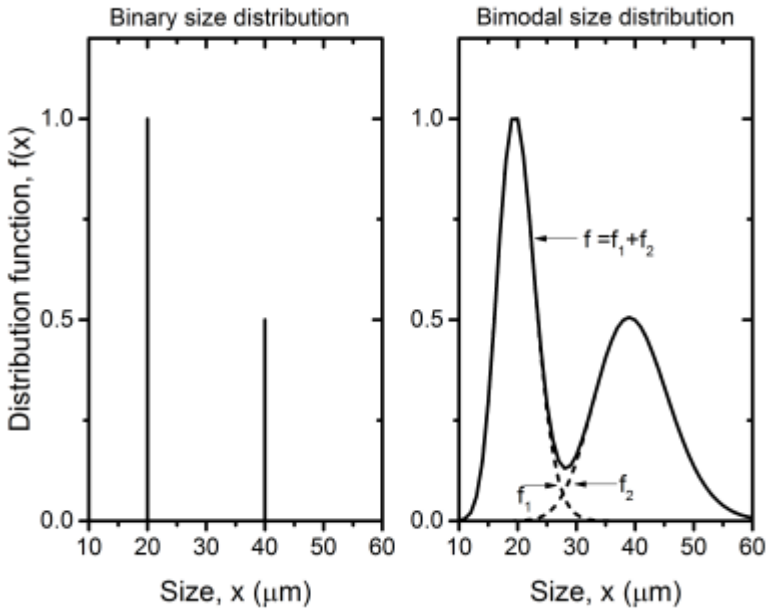

Fig. 1 A schematic depiction of the size distributions of a binary suspension (left) and bimodal suspension (right). For the bimodal size distribution, $f\left(x\right)$, the constituent unimodal suspensions, $f_1\left(x\right)$ and $f_2\left(x\right)$, are shown in dashed lines.

If we consider a binary suspension as a mixture of two monodisperse particle sizes (d and D) with total volume fraction ϕ, the viscosity of this suspension can be predicted once the constituent

monodisperse viscosity correlations for the individual particle size suspensions, $\eta_{r,d}(\phi)$ and $\eta_{r,D}(\phi)$, are known. Furthermore, for ideal non-colloidal suspensions, a simplification emerges as the monodisperse suspension viscosity is independent of size such that $\eta_{r,d}=\eta_{r,D}=\eta_r(\phi)$. The MWB model equations for the case of a binary suspension viscosity, $\eta_{r,bi}$, are provided by

$$\begin{aligned}
&\eta_{r,bi} \equiv \exp(f_{bi}) \quad \text{where} \\
&f_{bi} = f_u\left(\beta(\phi_d)^*_{d,D} + \phi_D\right) + f_u\left(\left(\frac{\phi_d}{(1-(1-\beta)\phi_D)}\right)^*_{d,D}\right)(1-\beta)\,, \\
&f_u(\phi) = \ln(\eta_r(\phi))\,, \\
&\beta \equiv \left[g\left(\frac{d}{D}\right)\right]^{h\left(\frac{\phi_d}{\phi_D}\right)}
\end{aligned} \quad . \tag{1}$$

In this expression, $f_u(\phi)$ is a hydrodynamic function defined based on the monodisperse viscosity correlation while β is a weighting function that depends on the relative size ratio d/D and composition of the constituents in the suspension such that $\phi=\phi_d+\phi_D$. A good choice for the weighting function is provided by

$$\begin{aligned}
&g\left(\frac{d}{D}\right) = \left(1-\left(1-d/D\right)^{0.9}\right)^{1.41} \text{ and} \\
&h\left(\frac{\phi_d}{\phi_D}\right) = \left(1.68\left(\frac{\phi_d}{\phi_d+\phi_D}\right)^2 - 2.01\left(\frac{\phi_d}{\phi_d+\phi_D}\right)+1\right)\left(1-\frac{2.5\phi_d}{2.5\phi_d+\phi_D}\right)
\end{aligned}\,, \tag{2}$$

developed in Mwasame *et al.* (2016a) based on fitting the MWB model to binary suspension viscosity data by of Chang and Powell (1994) and Chong *et al.* (1971).

The application of the MWB model to bimodal suspensions requires the two constituent unimodal size distributions to be coarse-grained such that one can define the corresponding relative sizes of the small and large particle constituents $d = d_1$ and $D = d_2$. This is accomplished by defining the d_i's as the volume weighted sizes of the constituent unimodal distributions. If $f_i(x)$ is represents a constituent unimodal number weighted size distribution with x the variable representing the size (in units of length), then the volume average size can be defined as

$$d_i = \frac{\int_0^\infty x^4 f_i(x)\,dx}{\int_0^\infty x^3 f_i(x)\,dx}\,. \tag{3}$$

In this way, a unimodally distributed suspension $f_i(x)$, with a volume fraction of ϕ_i is characterized as an equivalent monodisperse suspension of size d_i and volume fraction ϕ_i. Subsequently, a bimodal suspension (see Fig. 1) comprising of $f_1(x)$ and $f_2(x)$ unimodal suspensions (and volume fractions $\phi_d = \phi_1$ and $\phi_D = \phi_2$) is represented as an equivalent suspension with volume weighted sizes $d = d_1$ and $D = d_2$ and volume fractions $\phi_d = \phi_1$ and $\phi_D = \phi_2$. In this way a bimodal suspension is represented as an equivalent binary suspension allowing one to compute the viscosity of a bimodal suspensions similar to that of a binary suspension following the MWB model framework in Eq. (1). In a similar fashion, the viscosity of a trimodal suspension can be computed through the MWB model by treating it as an equivalent ternary suspension (Mwasame *et al.* 2016b) where the constituent unimodally distributed particle size distributions are coarse-grained following the approach described above. Note that subsequent extension of the MWB model to ternary, and in general multi-n-ary suspensions, does not introduce any new parameters such that the same weighting function β is defined through Eq. (1) and (2). Higher order multimodal suspensions can also be handled through the same scheme.

MATERIALS AND METHODS

Materials

The unimodal suspension were made using microspheres obtained from Potters Industries Incorporated with product identifications (PII) 150615E (11 µm), PII 602589 (38 µm) and PII 602587 (63 µm). The composition and densities of these particles are summarized in Table 1. Sigma-Aldrich Polyethylene glycol (PEG) MW 200 (0.045 Pa-s) was used as the suspending medium. The refractive index of the particles is approximately 1.51 and that of the PEG is 1.49 ensuring that London dispersion forces are minimized.

Table 1: Particles used and manufacturer reported specifications (diameter is number average).

Particle ID	Diameter (µm)	Specific Gravity	Composition
PII 603921	11	1.1	Borosilicate glass
PII 602590	38	2.5	Soda-lime glass
PII 602587	63	2.5	Soda-lime glass

Particle Size Measurements

The particle size distributions of the three particle types used in this study were obtained from images taken from a Nikon Eclipse TE2000-U microscope using the Canon EOS Rebel T1i camera. The images were analyzed using ImageJ software with a conversion of 13.5 pixels equal to one micron as determined using a micro-ruler. To get this pixel to micron conversion, an image of the micro ruler at the same magnification used to take pictures of the particles (40x) was used to set the scale. The size of the particles was determined from the projected areas in the images (see Fig. 3) by assuming a spherical shape. Having previously determined the scale, the oval/circle tool was used to enclose the area of the particle. Using the formula for the area of a circle, a radius for the particle can easily be determined and the size (diameter) and volume can also be calculated. 50 particles of each size were examined using this sizing regime and the average volume weighted size reported was calculated as the ratio of the fourth moment to the third moment (see Eq. (3)) of the experimentally constructed distributions. 50 particle measurements are sufficient to accurately determine the particle size as the F-test shows that the differences in the standard deviations are not statistically significant after at least 40 particles are sampled.

Density measurements

The effective densities of the unimodal particle suspensions used in all calculations in this work were independently measured using calibrated volumetric flasks with volumes of 10±0.02ml and 25±0.03ml. The density of the PEG is determined by simply weighing out a known volume of PEG in the volumetric flask using a micro-balance. Subsequently, the density of the particles in the suspensions is determined using the same method, with PEG as the dispersing medium.

Preparation of suspensions for rheological measurements

The suspensions used for the rheological measurements were prepared on a gravimetric basis based on the density measurements. After preparing stock solutions for each of the three unimodal suspensions at volume fractions of 0.55, the suspensions were placed in sealed 250 ml plastic bottles and placed on a roll mixer to ensure good mixing and subsequently placed in a vacuum oven for an hour to eliminate any air bubbles introduced during mixing. Subsequently, these stock solutions were diluted using PEG to nominal volume fractions of 0.1, 0.2, 0.3, and 0.45. To avoid propagating errors associated with serial dilutions, only direct dilutions from the stock solutions were carried out. Similarly, the bimodal and trimodal blends were also prepared from stock solutions using the same procedure described for the unimodal suspensions.

Rheological Measurements

Rheological measurements were performed using the TA AR2000 Rheometer in the stress-controlled setting. The geometry used for all experiments was a 40mm Aluminum Parallel Plate at a gap height of 500 μm. The experiments were run at 25 ^{o}C, with temperature control provided by use of a Peltier plate. The protocol used to collect the rheological data was to run 10 oscillatory stress sweep pre-shear cycles from 15 to 100 Pa at a frequency of 1 Hz before each peak hold test whose long time values are used to determine the reported steady state measurement used in the subsequent analysis. The peak hold experiments were run over a range from 15 to 100 Pa. Since some of the suspensions deviate from Newtonian behavior, only the peak holds at 25 and 75 Pa are reported in this paper with additional experimental data is presented in the supplementary material. The dynamic range for the shear stress is selected to ensure that the Shield's parameter[1] is kept relatively high (≥20) to mitigate the effects of settling (Zarraga et al. 2000). The effects of slip are not anticipated to be significant in the experiments carried out as the gap size is of order 10x the largest particle diameter. We also note that the measured viscosities of the three different unimodal noncolloidal suspensions are in good agreement with each other to within experimental uncertainty, which would not be the case were slip effects significant for the suspension with the largest particle size. Finally, whenever possible, random duplicate runs were carried out to ensure results were reproducible.

Experimental design

The experiments that were carried out were proposed based on two criteria: (1) to be informative such that the empirical unimodal viscosity correlations required to complete the MWB model can be determined and (2) to be extensive so that a reasonable number of combinations of compositions and size ratios (as indicated by the particle IDs-see table 1) is considered to allow for rigorous testing of the MWB model predictions. To fulfill these criterion, a rational experimental design is adopted and is summarized in the ternary plot of compositions and size ratios below in Fig. 2. In this diagram the vertices (star symbols) indicate the unimodal suspensions, prepared at total solids loadings, ϕ, of 0.1, 0.2, 0.3, 0.45 and 0.5. The boundaries of the ternary plot (circle symbols) correspond to the various compositions of the bimodal suspensions prepared at total solids loadings, ϕ, of 0.3 and 0.55. Finally, interior of the ternary plot (square symbols) correspond to the various compositions of the trimodal suspensions also

[1] The Shield's parameter Ψ is calculated as $\Psi = \tau/\Delta\rho g a$ where τ is the shear stress, $\Delta\rho$ is the difference in the density of the suspended particle and the suspension medium, g is gravitational acceleration and a is the radius of the particle.

prepared at total solids loadings, ϕ, of 0.3 and 0.55. The points on the vertices allow for criteria (1) as described above to be fulfilled while the rest of the points allow for the conditions of criteria (2) to be met.

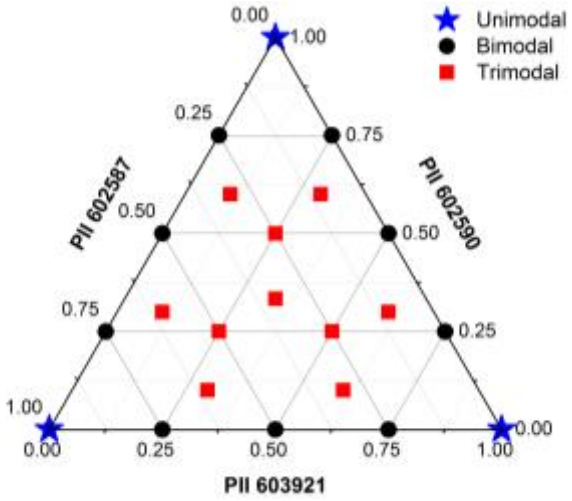

Fig. 2 A schematic showing all the combinations of composition and particle sizes (as indicated by the particle IDs) that were examined in this experimental study. Star symbols indicate monodisperse suspensions, circle symbols indicate bimodal suspensions and square symbols represent ternary suspensions that were considered in this work.

EXPERIMENTAL RESULTS AND DISCUSSION

Particle size and density determination

The calculated average volume weighted sizes and densities of the three unimodal suspensions are reported in Table 2. The volume weighted sizes in Table 2 are the 'representative sizes' that are used in the MWB model (and all subsequent discussions) as the characteristic average size of the unimodal suspensions in a specific bimodal or trimodal suspension (see appendix A for details on particle size distributions used to calculate these values). Representative snapshots of the images used to determine the particle size distributions are presented in Fig. 3. In addition, from the standard deviations of the number average sizes, the 60 µm particles are the most monodisperse, while the other two particle sizes have more significant polydispersity.

Table 2: Experimentally determined particle sizes and densities of the unimodal particles

Particle ID	Number average size (standard deviation) in µm	Volume weighted size in µm (2 significant figures)	Density (g/cm^3)
PII 603921	8.71 (4.12)	13	1.08±0.07
PII 602590	13.61 (6.96)	22	2.53±0.03

PII 602587	59.43 (2.28)	60	2.63±0.06

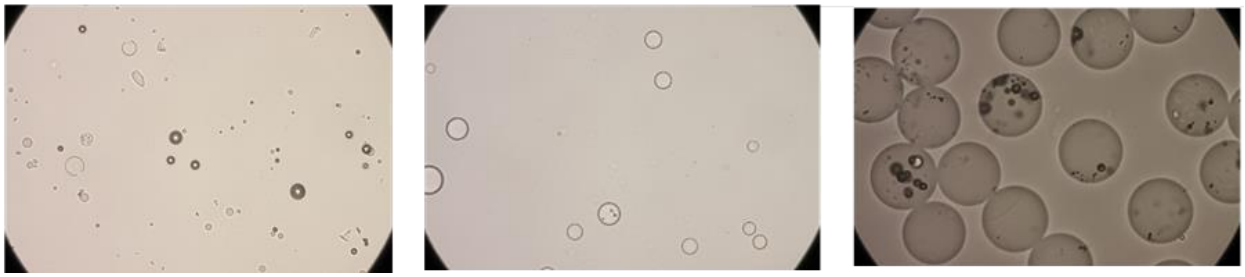

Fig. 3 Representative light microscopy images used in the ImageJ analysis to determine the particle size distributions. From left to right, the images correspond to particles with volume weighted average sizes of 13, 22 and 60 μm respectively (see table 2).

Unimodal suspension rheology

The viscosity behavior of the three unimodal suspensions is first studied as this is an important input to the MWB model. The rheological measurements were taken on the three unimodal suspensions (13, 22 and 60 micron volume average sized particles) at nominal volume fractions, ϕ, of 0.1, 0.2, 0.3, 0.45 and 0.55. The experimentally measured viscosities reported in Fig. 4 correspond to shear stresses of 25 and 75 Pa. It is interesting to note that among these formulations of non-colloidal suspensions, the 60 micron particles have the lowest viscosity despite having the least polydispersity (see table 2), suggesting additional interparticle forces or surface effects may be important. In the same figure, the solid blue line represents the fit of the Maron-Pierce equation (Maron and Pierce 1956)

$$\eta_r = \left(1 - \frac{\phi}{\phi_{\max}}\right)^{-2}, \tag{4}$$

to the average of the three experimentally measured unimodal suspension viscosities. The maximum packing fraction at both shear stresses is determined to be 0.58. These viscosity correlation fits to the average unimodal viscosity data are the same ones used in the MWB model to define $f_u(\phi) = \ln(\eta_r(\phi))$ (see Eq. (1)) and therefore facilitate the subsequent predictions of the bimodal and trimodal suspension viscosities at the two shear stresses considered in this work. We note that although Eq. (4) with a value of $\phi_{\max} = 0.58$ does not satisify the dilute limiting behavior derived by Einstein (1906, 1911), i.e., $\eta_r = 1 + 2.5\phi$. Indeed other, empirical relations that satisfy the dilute limiting behavior, such as the Kreiger-Dougherty equation, can also be used for correlating the unimodal suspension viscosities, as the

suspensions considered in this work are at relatively high volume fractions, this choice is unimportant for all the results that follow.

Finally, we clarify that despite the approach taken here to use an average viscosity across the three suspensions to represent the viscosity behavior of each unimodal suspension, in the general form of the MWB model (Mwasame *et al.* 2016b), one can define a different/independent viscosity function for each of the different size classes i, such that $f_u^i(\phi) = \ln(\eta_r^i(\phi))$, and therefore, avoid what is essentially a second coarse graining step. However, such rigor is not emphasized at this point owing to the uncertainty inherent in the volume fraction determination (see horizontal error bars and more information in appendix B). The possible consequences of such an assumption in performing model predictions will be evaluated in a later section. We also note that vertical error bars are not included as replicate experiments for select volume fractions were carried out (see supplemental section) showing the results reported in Fig. 4 are very reproducible.

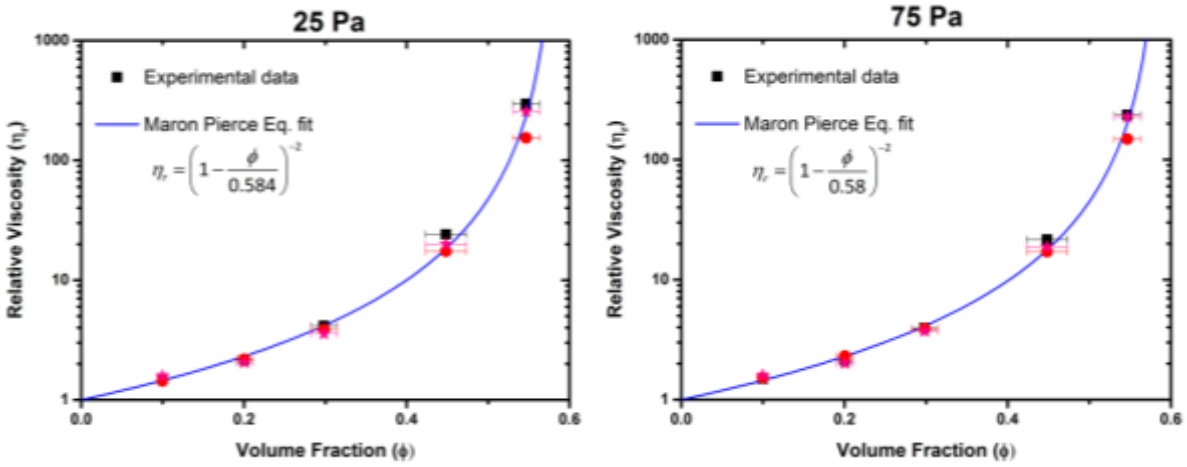

Fig. 4 The average relative viscosity as a function of the volume fraction at two shear stress values. The symbols represent the experimentally measured values of the relative viscosity while the solid line represents the fits of the average viscosity to the Maron-Pierce equation. Filled squares are 13 micron particles, filled circles are 22 micron particles and filled stars are 60 micron particles. The horizontal error bars correspond to the uncertainty in the volume fraction calculations determined through error propagation.

Bimodal suspension rheology and model predictions

The three unimodal suspensions with volume weighted sizes 13, 22 and 60 microns were blended to form three bimodal suspensions, 13-22, 13-60, and 22-60 microns, whose viscosities were measured at two total solids loadings, $\phi = 0.3$ and $\phi = 0.55$ and two different shear stresses (25 and 75 Pa). The bimodal experimental data, taken at different volume ratios of the constituent unimodal suspensions, is

summarized by the filled circles in Fig. 5. In the definition of the volume ratio as $0 \le \phi_d / (\phi_d + \phi_D) \le 1$, d and D are defined as the small and large volume weighted sizes of the two constituent unimodal particle size distributions that comprise the bimodal suspension. The experimental data show that blends of two unimodal suspensions have lower viscosity than the individual unimodal suspensions alone. Furthermore, most of the experimental data shows a viscosity minimum when the volume ratio is approximately between 0.25-0.5. These results are consistent with expectations (Mewis and Wagner 2012). The error bars shown in Fig. 5 are only representative and are estimated by assuming that the viscosity of the bimodal blends as a function of the volume ratio, $\phi_d / (\phi_d + \phi_D)$, holding the total volume fraction constant, obeys a quadratic relationship. Subsequently, the uncertainty in the viscosity measurements can be estimated from the experimental data and the quadratic fit to the data as

$$\sigma^2 = \frac{\sum_{i=1}^{N} \left(\eta_{i,\text{experiment}} - \eta_{i,\text{quadratic fit}} \right)^2}{N - d} \,. \tag{1.5}$$

In this expression, d is the number of degrees of freedom taken as 3 and represents the number of parameters in the quadratic fitting equation. The error bars reported on each panel of Fig. 5 corresponds to 2σ computed from the above formula using the experimental data in the same panel with $N = 5$.

The unimodal viscosity correlation and the volume weighted sizes are the only inputs required to use the MWB model in a predictive fashion and allow comparison against the bimodal suspension data. A detailed discussion of this aspect of the model equations is available in the literature (Mwasame *et al.* (2016a)). For simplicity, the unimodal viscosity correlation underlying subsequent MWB model predictions is that obtained by fitting Eq. (4) to the average viscosity data of the three unimodal suspensions, as shown in Fig. 5. The MWB model predictions for the three different bimodal suspensions are compared against experimental data in Fig. 5, and these are represented by the solid lines. The dashed lines indicate the prediction intervals computed based on the uncertainty in the volume calculations. Overall, the model makes reasonable predictions, capturing the effects of blending on suspension viscosity. We reiterate that in applying the MWB model to make these predictions, the mixed unimodal suspensions are characterized as equivalent monodisperse suspensions through their volume weighted sizes, which is used in determining the weighting functions that appear in the MWB model i.e., Eqs. (1) and (2).

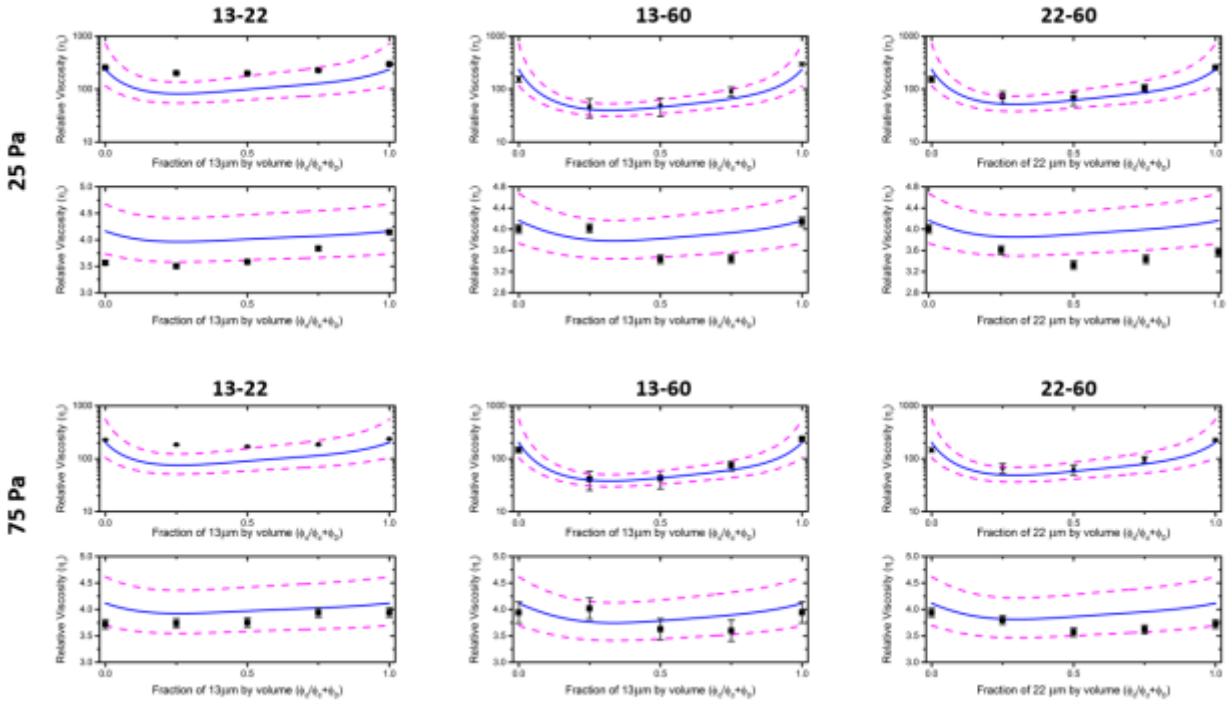

Fig. 5 A comparison of the predictions of the viscosity of the bimodal suspensions compared against experimental data, as the fraction of small particles by volume, $\phi_d/(\phi_d+\phi_D)$, is varied from 0 to 1. At each of the shear stresses shown, the total solids loading, ϕ, in the top row is 0.55, while in the bottom row it is 0.3. Also, d and D are defined as the small and large volume weighed sizes of the constituent unimodal particle size distributions that comprise the bimodal suspension. Solid lines are the model predictions, dashed lines represent prediction intervals based on the uncertainty in volume fraction measurements and symbols signify experimental data. See text for discussion on how error bars were estimated.

Trimodal suspension rheology and model predictions

The three unimodal suspensions with volume weighted sizes 13, 22 and 60 microns were also blended to form trimodal suspensions at 10 different compositions of the various constituent unimodal suspensions., Viscosities were measured at solids loadings of $\phi=0.3$ and $\phi=0.55$.. The resultant experimental data is summarized in Fig. 6 by filled square symbols and the composition of the different blends, labeled run 1 to 10 in the same figure are described in Table 3. At both shear stresses and solids loadings examined, there are no discernible trends (note the data at $\phi=0.3$ is on a linear y-scale while that at $\phi=0.55$ is on a log y-scale). However, at $\phi=0.55$, there are significantly larger variations in viscosity as the composition changes that can provide a stringent test on the capabilities of the MWB model.

The trimodal viscosity predictions of the MWB model (see Mwasame *et al.* (2016) for detailed equations) are compared against experimentally measured viscosities of the trimodal suspensions in Fig. 6. The model predictions are represented by open symbols, while the dashed lines are the prediction intervals based on the uncertainty in the experimental volume fraction calculations. In general, the model captures the qualitative and quantitative trends seen in experimental data and in all cases, the experimental data are essentially within the prediction interval of the model. Furthermore, the model uniformly predicts run 7 (see table 3) to provide the lowest viscosity. While this prediction is not corroborated by the experimental data at $\phi = 0.3$, it is clearly in agreement with experiments at $\phi = 0.55$ at both 25 and 75 Pa where the changes in viscosity are more significant. The ability of the MWB model to correctly capture the trends seen in the experimental data, especially at high volume fraction where the viscosity changes between compositions are large in magnitude, demonstrates its robustness and provides further credence to the coarse-graining methodology previously described. Finally we note the MWB model predicts the composition that results in the minimum viscosity of the trimodal suspension is 0.22:0.16:0.62, representing the fraction by volume of the 13:22:60 μm particles. The corresponding minimum relative viscosity at $\phi = 0.55$ is 37.5 while at $\phi = 0.3$ its value is 3.75. These results are consistent with our experimental observations at $\phi = 0.55$ of the lowest viscosity being observed in run 7 (see table 3) whose composition is 0.3:0.1:0.6.

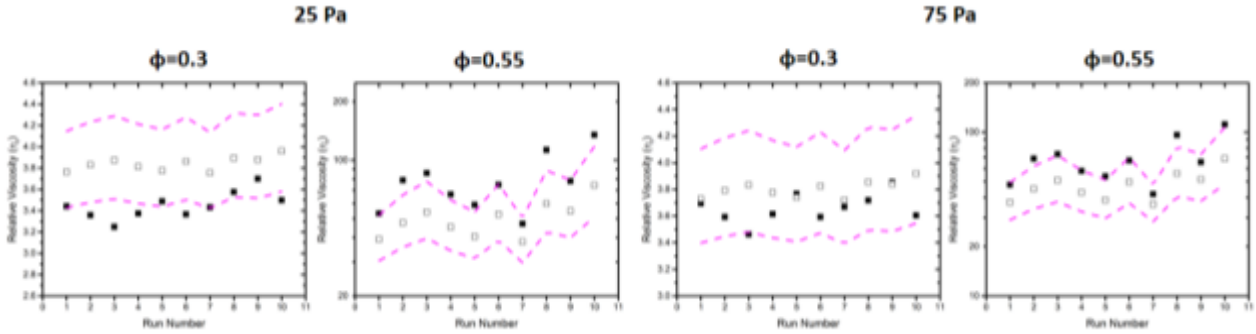

Fig. 6 A comparison of the predictions of the viscosity of the trimodal suspensions compared against experimental data (filled square symbols) at different compositions of small, intermediate and large particles (see Table 3 for interpretation of run number). At each of the shear stresses shown, two total solids loadings at 0.3 and 0.5 are examined. Open symbols are the model predictions, dashed lines represent prediction intervals based on uncertainty in volume fraction measurements and filled symbols signify experimental data. Note at $\phi = 0.3$, the data is presented on a linear y-scale while at $\phi = 0.55$ it is presented on a log y-scale.

Table 3: The composition of the trimodal viscosity blends comprised of three unimodally distributed size distributions.

Run number	Fraction by volume of 13:22:60 μm particles
1	0.25:0.25:0.5
2	0.25:0.5:0.25
3	0.5:0.25:0.25
4	0.33:0.33:0.33
5	0.1:0.3:0.6
6	0.1:0.6:0.3
7	0.3:0.1:0.6
8	0.3:0.6:0.1
9	0.6:0.1:0.3
10	0.6:0.3:0.1

An examination of the modeling assumptions

Although the main focus of this paper is the application of the MWB model in the context of an engineering approach, it is important to evaluate one of the coarse graining assumptions to reveal the true capabilities of the MWB model. A key approximation in discussion so far is the use of a single average viscosity correlation to represent the unimodal suspension behavior when applying the MWB model. From Figs. 5 and 6 it is apparent that the approach does a reasonable job in capturing the experimental data to within experimentally expected uncertainty. On the other hand, from Fig. 4, it is clear that the three blended unimodal suspensions do not strictly obey the same universal viscosity correlation. Fortunately, the MWB model is also capable of being used in a predictive fashion if the unimodal suspensions viscosity correlations obeyed by the blended particles sizes are treated differently (Mwasame *et al.* 2016b). In this section, we examine the implications of employing much better fits of the individual unimodal suspension behavior towards predicting the observed bimodal suspension behavior of the 13-22 particle blends at a shear stress of 75 Pa. The data on the unimodal suspensions behavior for these two particle sizes, 13 and 22 microns, in Fig. 7, are fit to the Mooney equation (Mooney 1951), which best represents, the data and given by the functional form

$$\eta_r = \exp\left(\frac{a\phi}{1-b\phi}\right). \tag{1.6}$$

For the unimodal particles with a volume average size of 13 microns, a=2.78 and b=1.30 while for the 22 micron sized particles, a= 2.57 and b=1.34. This completes the information required to predict the bimodal suspension data through the MWB model. The subsequent predictions of the bimodal suspension data

are presented in Fig. 8, and these are compared against the result arising from the previous assumption that 13 and 22 micron unimodally distributed particles obey the same correlation as presented in Eq. (4) (as depicted in Fig. 4). It is clear that treating the individual unimodal particle viscosity correlations independently yields much better quantitative agreement with experiments. In addition, by also fitting the 60 micron particles unimodal suspension viscosity to Eq. (4) with $\phi_{max} = 0.6$, the trimodal suspension viscosity behavior can also be predicted using the same scheme with greater overall fidelity at higher volume fraction ($\phi = 0.55$), as shown in Fig. 9. These two examples show that explicitly accounting for the individual unimodal suspension viscosity correlations enables better predictions of the measured experimental data than employing a single average viscosity correlation. In this way, the capability of the MWB model to allow for independent viscosity correlations provides additional robustness to apply the model to predict the overall viscosity of mixtures whereby the suspension behavior of the individual components is non-ideal (Mwasame *et al.* 2016b).

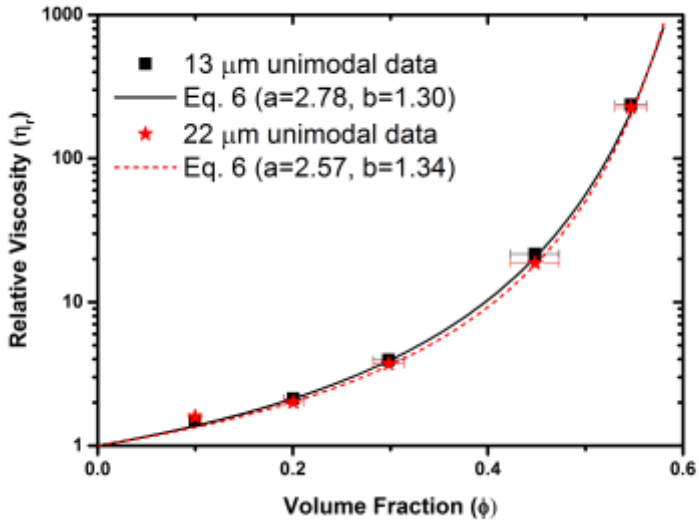

Fig. 7 The average relative viscosity as a function of the volume fraction at a shear stress value of 75 Pa for the 13 and 22 micron particles by volume weighted size. The symbols represent the experimentally measured values of the relative viscosity while the solid line represents the corresponding fits to the Mooney equation. The horizontal error bars correspond to the uncertainty in the volume fraction calculations from error propagation.

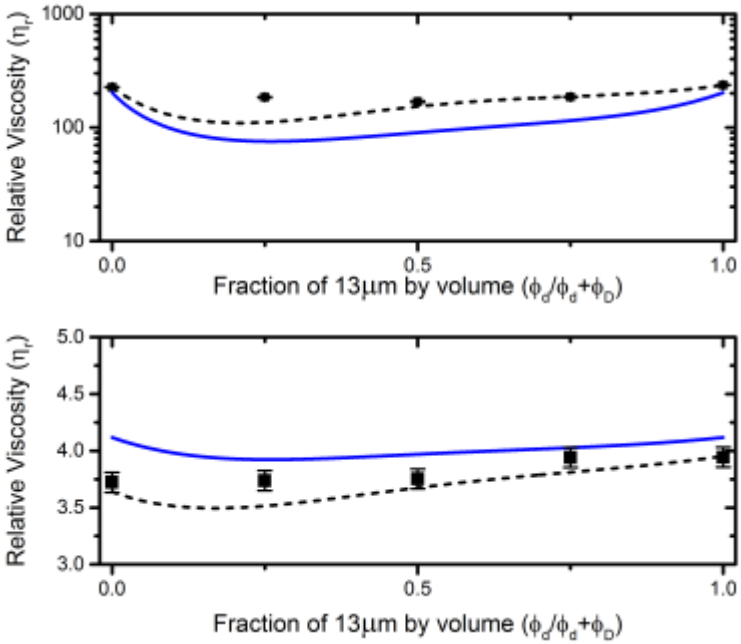

Fig. 8 A comparison of the predictions of the viscosity of the 13-22 bimodal suspension compared against experimental data (at a fixed shear stress of 75Pa), as the fraction of small particles by volume, $\phi_d/(\phi_d+\phi_D)$, is varied from 0 to 1. The total solids loading, ϕ, in the top row is 0.55, while in the bottom row it is 0.3. Also, d and D are defined as the small and large volume weighed sizes of the constituent unimodal particle size distributions that comprise the bimodal suspension. Solid lines are the MWB model predictions using a single viscosity correlation to represent the unimodal suspension data (as appearing in Fig. 5) while dashed line represents model predictions using independent viscosity correlations for the two unimodal suspensions based on Fig. 7.

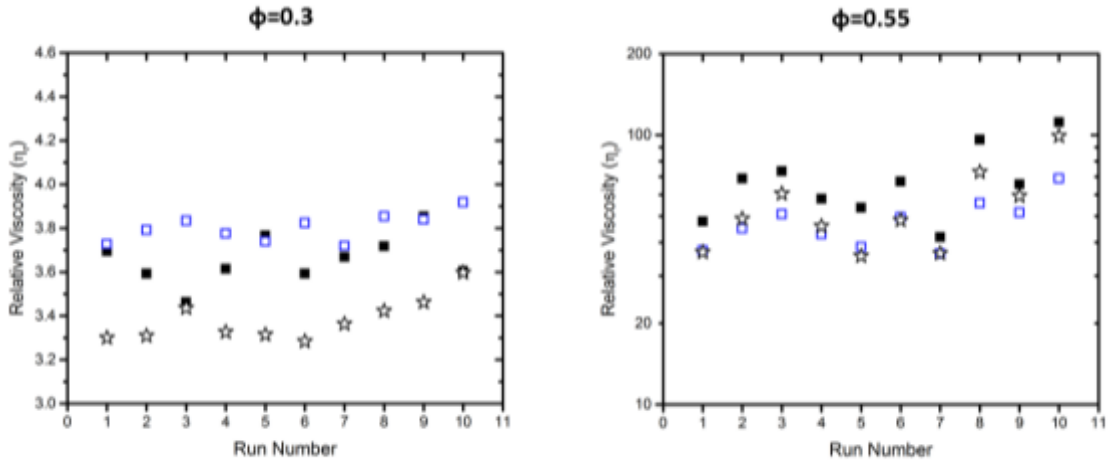

Fig. 9 A comparison of the predictions of the viscosity of the trimodal suspensions compared against experimental data at 75 Pa (filled square symbols) at different compositions of small, intermediate and large particles (see Table 3 for interpretation of run number). Open square symbols are the MWB model predictions using a single viscosity correlation to represent the unimodal suspension data (as appearing in Fig. 6) while dashed line represents model predictions using independent viscosity correlations for the three individual unimodal suspensions viscosity correlations (see text).

CONCLUSION

Viscosity measurements of unimodal suspensions and their bimodal and trimodal mixtures provide a new experimental dataset that is used to validate a leading model that is rigorously consistent in treating multicomponent suspensions within effective medium theory. The large experimental state space allows for a rigorous testing of the MWB model. Good agreement of MWB predictions with measurements for bimodal and trimodal mixtures is observed, where the highly nontrivial dependence of the viscosity for trimodal suspensions is accurately captured by the MWB model with only the unimodal viscosity functions and volume average sizes provided as input. This model is shown to be accurate for "interfering" size ratios. The semi-empirical nature of the MWB model (i.e., only requiring independent measurement of the constituent unimodal or monodisperse suspension viscosity to make predictions) likely explains the relative success experienced here as any suspension- dependent features are implicitly taken into account, rendering the MWB model robust.

Another key outcome of this work is that unimodal suspension behavior can be treated within the context of the MWB model as monodisperse if the unimodal suspension is characterized by its volume weighted average size. This coarse-graining is an engineering approach that may be a useful starting point, in general, towards extending the applicability models and theories based on monodisperse size distributions to systems that possess a broad, or multimodal size distribution. Based on this extensive comparison with experiment, we conclude that the MWB model shows promise towards predictive modeling of the viscosity of industrially relevant suspensions and therefore, may be useful for optimizing flow properties at high solids loading by blending suspensions.

Acknowledgements

This material is based upon work supported by the National Science Foundation under Grant No. CBET 312146. Any opinions, findings, and conclusions or recommendations expressed in this material are those of the author(s) and do not necessarily reflect the views of the National Science Foundation.

References

Chang, C, Powell RL (1994) Effect of particle size distributions on the rheology of concentrated binary suspensions. J Rheol 38:85–98

Chong, JS, Christiansen EB, Baer AD (1971) Rheology of concentrated suspensions. J. Appl. Polym. Sci. 15, 2007–2021

Dörr A, Sadiki A, Mehdizadeh A (2013) A discrete model for the apparent viscosity of polydisperse suspensions including maximum packing fraction. J Rheol 57:743–765

Einstein A (1906) A new determination of molecular dimensions. Ann. Phys. 324:289–306

Einstein A (1911) A new determination of molecular dimensions. Ann. Phys. 339: 591–592

Faroughi SA, Huber C (2014) Crowding-based rheological model for suspensions of rigid binary-sized particles with interfering size ratios. Phys Rev E 90:052303

Farr RS (2014) Simple heuristic for the viscosity of polydisperse hard spheres. J Chem Phys 141:214503

Farris RJ (1968) Prediction of the viscosity of multimodal Suspensions from monodisperse viscosity data. Trans Soc Rheol 12:281-301

Furnas CC (1931) Grading aggregates-I—Mathematical relations for beds of broken solids of maximum density. Ind Eng Chem 23:1052–1058

Maron SH, Pierce PE (1956) Application of ree-eyring generalized flow theory to suspensions of spherical particles. J Colloid Sci 11:80-95

Mewis J, Wagner NJ (2012) Colloidal suspension rheology. Cambridge University Press

Mooney M (1951) The viscosity of a concentrated suspension of spherical particles. J Colloid Sci 6:162-170.

Mwasame PM, Wagner NJ, Beris AN (2016a) Modeling the effects of polydispersity on the viscosity of noncolloidal hard sphere suspensions. J Rheol 60:225–240

Mwasame PM, Wagner NJ, Beris AN (2016b) Modeling the viscosity of polydisperse suspensions: Improvements in prediction of limiting behavior. Phys Fluids 28: 061701

Ouchiyama N, Tanaka T (1984) Porosity estimation for random packings of spherical particles. Ind. Eng. Chem. Fundam. 23:490–493

Qi F., Tanner R. (2012) Random close packing and relative viscosity of multimodal suspensions. Rheologica Acta 51:289-302

Shewan HM, Stokes JA (2015) Viscosity of soft spherical micro-hydrogel suspensions. J Colloid Interface Sci 442:75-81

Wagner NJ, Woutersen AM (1994) The viscosity of binary and polydisperse suspensions of hard spheres in the dilute limit. J. Fluid Mech. 278:267–287

Zarraga IE, Hill DA, Leighton DT (2000) The characterization of the total stress of concentrated suspensions of noncolloidal spheres in Newtonian fluids. J Rheol. 44**:**185-220

Appendix A

This appendix summarizes the data on the experimentally determined particle size distributions. The data in Table A1 correspond to the sizes determined from the microscopy images processed using ImageJ software. The volume weighted average sizes reported in Table 2 are computed from this data.

Table A1: Summary of particle sizes in a sample of 50 particles determined from processing microscopy images using ImageJ software.

	Particle sizes in μm				Particle sizes in μm		
No.	PII 603921	PII 602590	PII 602587	No.	PII 603921	PII 602590	PII 602587
1	6.07	4.40	57.80	26	9.70	6.88	60.47
2	5.88	9.07	59.47	27	12.55	6.44	51.68
3	12.60	10.58	60.39	28	6.84	6.03	63.30
4	13.03	14.73	58.17	29	11.81	3.93	62.93
5	9.65	14.62	59.03	30	8.48	3.29	56.97
6	16.17	11.92	58.43	31	9.91	12.32	58.50
7	5.03	12.99	61.95	32	10.62	13.51	60.96
8	4.26	15.13	58.77	33	4.40	8.48	58.46
9	4.55	15.69	60.99	34	5.85	12.29	59.80
10	14.17	19.72	60.54	35	3.81	20.28	58.13
11	3.45	19.58	57.77	36	5.48	5.29	61.03
12	4.92	26.01	63.36	37	5.14	4.33	60.02
13	8.44	25.05	58.47	38	5.32	26.64	58.72
14	6.78	22.87	60.76	39	5.26	3.75	59.62
15	3.78	14.21	58.62	40	4.74	7.10	61.70
16	4.07	16.06	56.25	41	4.66	7.22	56.71
17	17.21	18.54	58.55	42	6.29	13.91	63.23
18	17.32	10.74	59.80	43	11.26	18.21	60.70
19	9.92	12.10	57.88	44	7.88	10.70	63.19
20	14.76	10.51	56.06	45	12.55	8.33	62.15
21	17.62	15.98	59.54	46	4.40	23.91	60.40
22	11.48	25.68	59.39	47	10.92	10.18	58.20
23	13.10	9.51	62.21	48	4.59	20.95	59.28
24	10.47	9.58	58.62	49	13.43	30.79	54.47
25	6.44	8.10	60.13	50	8.70	22.51	57.98

Appendix B

This appendix summarizes the calculations used to determine the volume fractions, density and error bars in Fig. 3. The values of the volume fraction reported in this paper are nominal volume fractions. This section describes the process by which error was propagated to obtain the unimodal viscosity correlations in Figure 2. For accuracy, all the suspensions were prepared on a gravimetric basis to ensure maximum accuracy. The determination of the error in the volume fractions starts with determining the density of the particles and PEG-200 medium. For this, volumetric flasks with a given uncertainty as well as a Fisher Scientific analytical balance were used. By determining the densities of the particles and medium by carrying out multiple replica experiments, the density and the associated error in its value is determined—see Table B1. Knowing the uncertainty in the micro-balance measurements as well as the density measurements on both the PEG-200 and the particles allowed for error to be further propagated to the level of the volume fractions at the stock solutions and the subsequent dilutions of the stock solution. The individual errors propagated for the volume fraction result in the horizontal error bars—see last 2 columns of Table B2.

Table B1: Summary of density and error for the three unimodally distributed particle sizes. The reported error is 95% confidence interval.

Unimodal particle distributions	Density	
	Value	Error
13 µm	1.08	0.07
22 µm	2.53	0.03
60 µm	2.63	0.06

Table B2: Summary of volume fractions for the three unimodally distributed particle sizes. Error in volume fraction is propagated from uncertainty in density and micro-balance measurement.

Nominal volume fractions	Unimodal particle distributions						Average	
	13 µm		22 µm		60 µm			
	Value	Error	Value	Error	Value	Error	Value	Error
ϕ=0.1	0.105	0.003	0.099	0.013	0.096	0.008	0.100	0.005
ϕ=0.2	0.211	0.006	0.199	0.019	0.192	0.024	0.201	0.01
ϕ=0.3	0.309	0.007	0.296	0.041	0.289	0.026	0.298	0.016

ϕ=0.45	0.462	0.011	0.446	0.046	0.437	0.058	0.448	0.025
ϕ=0.55	0.557	0.011	0.547	0.035	0.537	0.034	0.547	0.016